Geological Quarterly, 2025, 69, 64
DOI: https://doi.org/10.7306/gq.1837

On the provenance of monazite and ilmenite from the Sea of Azov coastal placers in Novopetrivka, Berdiansk Region, Zaporizhzhia Oblast, Ukraine

Adam PIESTRZYŃSKI[1, *], Ihor NIKITENKO[2], Gabriela KOZUB-BUDZYŃ[1] and Serhii SHEVCHENKO[2]

[1] AGH University of Krakow, al. Mickiewicza 30, 30-059 Kraków, Poland; ORCID: 0000-0001-6649-6772 [A.P.], 0000-0002-3489-9822 [G.Z.-B.]

[2] Dnipro University of Technology, Dmytra Yavornytskoho Ave, 19, Dnipro, Dnipropetrovsk Oblast, Ukraina, 49005

Piestrzyński, A., Nikitenko, I., Kozub-Budzyń, G., Shevchenko, S., 2025. On the provenance of monazite and ilmenite from the Sea of Azov coastal placers in Novopetrivka, Berdiansk Region, Zaporizhzhia Oblast, Ukraine. Geological Quarterly, **69**, 64; https://doi.org/10.7306/gq.1837

Associate Editor: Karol Zglinicki

The primary source of economically important coastal sand minerals has been identified. Monazite and ilmenite, which occur in the vicinity of Berdiansk city on the northern coast of the Sea of Azov in Ukraine, and determine the possibility of their practical use. The chemical and mineral composition of the placer minerals, their textural characteristics and radiometric ages help in determining their origin. Monazite from the coastal black sands of Novopetrivka is of Paleoproterozoic age. Thorium-bearing monazites of this age are a typical accessory mineral of the Anadolskyi, Saltychanskyi and Kamianomohylskyi granitoid complexes of the Pryazovskyi megablock of the Ukrainian Shield. The ilmenites are of various origins. The deposits of both monazite and other minerals of the black sands, common in the beach zone near the village of Novopetrivka, were predominantly formed from terrigenous material brought earlier by rivers from the Pryazovskyi megablock area. The monazites examined from the northern zone of the Sea of Azov are characterized by significant neodymium, samarium, europium, gadolinium, terbium and dysprosium contents, reaching up to 14 wt.% (as oxides). Apart from monazites, ilmenite, garnet and fine-grained quartz can be good economic targets.

Key words: monazite, ilmenite, coastal sands, Sea of Azov, Ukraine.

INTRODUCTION

Monazite- and ilmenite-bearing black sands have long been of special geological interest. Firstly, because of the economic value of both minerals. Ilmenite sands are the main source of titanium, while monazite contains thorium, uranium as well as rare earth elements such as cerium and lanthanum. Secondly, monazite is a radioactive mineral widely used in radiometric dating. This makes it possible to ascertain the age of both crystalline and sedimentary rocks. Therefore, it is important not only for structural geology, but also for studies of sedimentary deposits.

There is currently much research into monazite-containing black sands. Recent performed studies include the genesis and evaluation of heavy minerals in black sands of the southern Eastern Desert of Egypt (Khedr et al., 2023). Itano et al. (2020) proposed a new approach to the quantitative discrimination of detrital monazite from different sources in sediments of African rivers, founded on machine-learning-based approaches. Anita et al. (2020) studied the distribution of monazite-bearing sands along the coast of the Neendakara – Kayamkulam belt, Kerala, India, as influences on their potential applications in the future. Chalmers et al. (2024) determined the provenance of Copi North heavy mineral sands deposit, Murray Basin, Australia, based on the geochronology and geochemistry of detrital zircon, rutile and monazite. Lithological research on the formation of detrital sediments in NW Denmark determined a connection between grain-size distribution and the heavy-mineral assemblages (Feil et al., 2024).

Today in Ukraine some placer deposits of titanium and associated minerals are exploited on a large scale. The studies are mainly focused on more efficient extraction of all the useful components and on ecological issues (e.g., Lozhnikov et al., 2023).

The history of research into the monazite-containing black sands of the northern coast of the Sea of Azov goes back about a hundred years, being especially prominent in the 1920s–1980s. During this period these sediments were studied by many authors (Chirvinskiy, 1925; Panteleyev, 1935; Savych-Zabolotskyi, 1937, 1939; Kariakin, 1948; Inozemtsev, 1974, 1975a, b; Shniukov et al., 1974, 1983). A renewal of interest began in 2010s, with studies published by Kovalchuk (2012), Dunets (2014), Poliashov et al. (2015), Stefanko (2018) and Shniukov et al. (2019).

* Corresponding author, e-mail: piestrz@agh.edu.pl

Received: July 4, 2025; accepted: December 16, 2025; first published online: January 12, 2026

In this study, we constrain the primary source of the placer minerals in the monazite-containing black sands in the village of the Novopetrivka, Berdiansk district, and ascertain the possibility of their use.

GEOLOGICAL SETTING

Chirvinskiy (1925), who studied these black sands, did not mention monazite. Panteleyev (1935) who regarded the black sands of the Azov Sea area as a promising source of titanium, performed mineralogical determinations of the sands and identified nine alluvial deposits of titanium-bearing (ilmenite) sands; he was the first researcher to measure the radioactivity levels in these sands and their possible content of thorium and zirconium. Savych-Zabolotskyi (1939) provided the first broad characterization of these black sands, identifying monazite among other minerals. Using petrographic techniques he established that, between the cities of Mariupol and Berdiansk, the sands include quartz, graphite, anatase, baddeleyite, zircon, ilmenite, magnetite, kyanite, garnet, hornblende, augite, staurolite, allanite, feldspars, mica (biotite and muscovite), titanite and monazite, while ilmenite was identified as the main placer ore mineral in the coastal zone to the west of Mariupol. Savych-Zabolotskyi (1939) attributed the origin of these modern placers to surf zone erosion and sorting of unconsolidated sediments that accumulated in Pontic time when erosion of terrigenous material from the mainland was more active. He regarded the Paleogene deposits of the Donbas as an initial source of staurolite, disthene and sillimanite. The other minerals, according to him, originated partly from the Pryazovskyi megablock of the Ukrainian Shield and partly from the volcanic rocks exposed along the rivers Krynka, Big and Small Nesvetai (Savych-Zabolotskyi, 1937, 1939), which were first described by Morozewich (1898). Savych-Zabolotskyi (1939) considered the Volnovakha alkaline massif located in the upper stream of the Kalchyk River and its tributary Kalmius (Fig. 1) to be the primary source of the monazite, together with zircon and badde-

Fig. 1. Geological sketch of the northern coast of the Sea of Azov (Pre-Quaternary formations)

K-N – Cretaceous-Neogene, AR-PR – Archean-Proterozoic (after Lazarenko, 1981, revised)

leyite. He associated the provenance of the ilmenite with amphibolites, which are common in the Northern Azov Sea area (Savych-Zabolotskyi, 1937, 1939). The work of Kariakin (1948), carried out after the end of World War II, was devoted to the practical use of these sands. As related by residents of the village of Novopetrivka, commercial mining of the black sands had taken place in the past, though with no record of the purpose for which it was used.

Logvinenko et al. (1964) determined the pattern of changes in the mineral composition of sands in different zones of the entire coast of the Sea of Azov. In particular, they linked the Berdiansk terrigenous-mineralogical province to the garnet-ilmenite-amphibole composition of black sands between the Liapina (east from Mariupol) and Fedotova (close to Crimea) spits. Monazite was not mentioned in the composition of the sands of the province and, probably, belonged to the category of other minerals (Logvinenko et al., 1964).

The monographs of Shniukov et al. (1974, 1983) were devoted to the geology and mineral resources of the Sea of Azov, and also considered the formation and distribution of placers in the bottom sediments. The black sands of the Azov Sea area were considered in the doctoral thesis of Inozemtsev (1974). He referred the Berdiansk terrigenous-mineralogical province, indicated by Logvinenko et al. (1964), to the North-Azov garnet-epidote-ilmenite-amphibole province, which included, in particular, the Berdiansk sub-province. According to Inozemtsev (1974), the source of the coastal sediments that occur in the central part of the northern coast is mainly from the products of erosion of crystalline rocks of the Azov Precambrian massif. He explained the diversity of the mineral composition by the close location of sources of drift deposits. Taking into account the fact that modern rivers, except for the Don and Kuban, scarcely carry any terrigenous material into the sea, Inozemtsev (1974), like Savych-Zabolotskyi (1939), associated the formation of modern placers with the erosion of Quaternary and Neogene deposits that underlie the main sea coast. These deposits were referred to the Lower Chaudin and Old Euxinian terraces developed along the northern coast of the Sea of Azov (Inozemtsev, 1975a, b). In addition to the beach area, Inozemtsev (1975b) noted the concentration of heavy minerals on the offshore slope and the tidal banks of underwater shafts, which, according to his data, are richer.

There has been a recent return of interest in the black sands of the Azov Sea area, which includes a different focus of work, towards solutions to environmental problems. In this respect, Kovalchuk (2012) studied the black sands in the area of village of Urzuf, in the Donetsk Oblast, and considered the sands as a promising source of titanium ore. Dunets and Poliashov (2014) studied the sandy deposits in the mouth of the Berda River and the possibilities of their processing. In addition, Poliashov (2015) with co-authors studied the radioactivity of the beach sands in the area of Berdiansk as regards potential harm to holidaymakers. Stefanko (2018) explored the primary source of the black sands of the beach area between Berdiansk and Mariupol, assessing the rock complexes of the Pryazovskyi megablock of the Ukrainian Shield as containing sufficient of the main minerals to be a source of the placer and including comparisons of the morphology of the monazite crystals. The possibility of fluvial sedimentary supply by the rivers running into the Sea of Azov, and the marine current directions, were also taken into account. As a result, the main sources of the black sands placer minerals were identified as granites of the Anadolskyi and Kamianomohylskyi complexes, which are widespread in the Eastern Azov Sea area (Stefanko, 2018). Shniukov et al. (2019) investigated the composition of the sands from the Obytichna Spit in the city of Prymorsk, west of Berdiansk, expanding the list of minerals of these coastal sandy deposits and identifying a group of minerals of technogenic origin. They noted the poverty of monazites and therefore of thorium in the area, which explains the lower level of radioactivity in the local sands (Shniukov et al., 2019).

METHODS

Analyses of monazite and ilmenite in coastal black sand deposits in the Novopetrivka area were performed on samples collected on the beach near the estuary of the Berda River and in the riverbed itself (Figs. 2 and 3). The sands were enriched in the Center of Processing and Beneficiation of Mineral and Technogenic Raw Materials of the Dnipro University of Technology (Dnipro, Ukraine). The black concentrate samples were examined in the Critical Elements Laboratory of the Faculty of Geology, Geophysics and Environmental Protection, AGH University of Krakow, Poland, where monazite and ilmenite were separated and investigated, and where microprobe analyses were also carried out using a *JEOL SQ8200*, operated in the wavelength-dispersion mode at an accelerating voltage of 20 kV, and a probe current of 40 nA, with a focused beam diameter of 1 m.

Fig. 2. The narrow branch of the Berda River flowing into the Sea of Azov in the village of Novopetrivka, east of Berdiansk (photo taken in 2019)

Fig. 3. Beach sands rich in garnet, quartz, ilmenite and monazite of the Sea of Azov, close to the estuary of the Berda River

Concrete reinforcement in right top corner of the photo (taken 2019)

The following standards and measurement lines were used for the monazite: SiK (albite), AlK (kyanite), SK (anhydrite), UM (UO_2), YL (YPO_4), PK (YPO_4), ScK (100%), TiK (rutile), CeL ($CePO_4$), LaL ($LaPO_4$), ThM (ThO_2), CaK (wollastonite), PrL ($PrPO_4$), TbL ($TbPO_4$), DyL ($DyPO_4$), ErL ($DyPO_4$), LuL ($LuPO_4$), GdL ($GdPO_4$), PbM (crocoite), NdL ($NdPO_4$), SmL ($SmPO_4$), EuL ($EuPO_4$), TmL ($TmPO_4$), YbL ($YbPO_4$), HoL ($HoPO_4$), AsL (InAs). Overlap correction of Nd-Ce, Sm-Ce, Lu-Dy, Dy-Eu, U-Th, Tm-Sm, Gd-Ho were implemented using the method described by Pyle et al. (2002).

For basic measurements, the following conditions were implemented: accelerating voltage of 15 kV, and a probe current of 40 nA, with a focused beam diameter of 3 m; counting times peak/background (in sec.) were as follows: Si 10/5, Al 10/5, S 20/10, U 120/60, REE 45/15, P 20/10, Ti 20/10, Th 120/60, Ca 20/10, Pb 180/90, V 10/5, Fe 20/10 and As 20/10. Original Jeol ZAF procedures were used for a final correction of all measured elements. The following crystals and standards were used: Fe K LIF (pyrite); Zn K LIF (sphalerite); In L PETJ (InAs); Mn K LIFL (MnS); Cd L PETL (greenockite); Hg M PET (HgTe); Cu K LIF (chalcopyrite); Ge L TAPH (GeS); As L TAPH (InAs); Sb L PETJ (stibnite); Ni K LIFH (Ni 100% metal.); Co K LIFL (Co 100% metal.); Pb M PETL (galena); Bi M PETL (bismuthinite); Ga L TAPH (GaP).

RESULTS

MONAZITE

Heavy sands were collected because of their elevated radiation, documented during the fieldwork in 2019. The monazite and ilmenite were collected from the coastal placers near the village of Novopetrivka (Fig. 1) in the middle of the 20th century. Gamma dose measurements showed that the beach sand near Novopetrivka emits low radiation levels, close to 0.2–0.3 Sv on average. However, the radioactivity of the monazite itself is much higher, reaching 25 kBq/kg (calculated from the average U content in monazite, cf. Table 1). Monazite was identified using both optical and electron microscopes (Fig. 4A–H).

In transmitted light, the monazites are seen as well-rounded grains, inhomogeneous and cloudy. The BSE images reveal their internal structure, most grains show clear zoning visible because of different thorium contents (Fig. 4; Appendix 1A: points 50–58, Fig. 4H), the white field within the monazite grain illustrated having the highest Th content (13.404 wt.%).

The chemical compositions of the monazites are given in Appendices 1A, B. The grains analysed are characterized by highly variable thorium contents ranging between 2.36 and 13.40 wt.% (Fig. 4 and Appendix 1). Straight boundaries between zones with different Th contents (Fig. 4) reflect changes in the composition of the mineralizing solutions. The difference can reach 5 wt.% (Appendix 1A: no 3 and 4). The monazites contain up to 65.198 wt.% of REE. The highest REE concentrations are related to the low thorium contents (Appendix 1A). Within the group of REE, the LREE are dominant (Fig. 5; Appendix 1B). Europium shows the lowest levels in this group (Appendix 1B). The two dominant elements are cerium and lanthanum, while average neodymium contents reach 10%. Apart from europium, all other elements are characterized by the low coefficient of variability (Appendix 1B). The HREE group is represented in the composition of monazites by only 0.637 wt.% with an average 0.356 wt.% for n = 61. For this REE group only Tb and Dy are present in quantities that allow for effective measurement using EMPA

The calculated monazite ages are very variable (Table 1), as indicated by a high standard deviation close to 100 Myr. However, the histogram of 61 measurements is similar to a Gauss curve (Fig. 6). Calculated ages reveal high variability within the individual grain (Table 1), which are optically correlated with BSE contrasted images.

ILMENITE

Ilmenite is one of the most common heavy minerals in the beach sand association analysed (Fig. 7). Ilmenite occurs in two different forms. Most common are individual grains, usually well-rounded, while angular grains are rare. Ilmenite occurred also in the form of lamellae and minute lenses in magnetite (Fig. 7A, C). These two different forms of ilmenite occurrence may indicate its origin from two or more different sources. Lamellae of magnetite in ilmenite have been detected in small quantities (Fig. 7C). Some of the ilmenite grains investigated show hydrothermal alteration in varying degrees of development (cf. Fig. 7B, D). The final product of such a process is anatase, clearly visible under the optical microscope because of its pale yellowish internal reflection (Fig. 7B, D).

The chemical composition of the ilmenites shows an almost stoichiometric composition (Table 2). The major constituents, Fe and Ti, are characterized by a low value of the variability coefficient, of 4.14 and 6.24% respectively. The ilmenites analysed reveal interesting admixtures of V_2O_5, MnO and MgO 0.20 wt.%, 2.91 wt.%, 0.247 wt.% respectively (Table 2). The highest variability among these elements shows manganese ranging from 0.32 to 9.181 wt.% (Table 2) with 51.33% of variability, for n = 34. Some analytical points show elevated amounts of Mn, close to 8–9 wt.%.

By comparison, ilmenite from the Krzemianka deposit (NE Poland, anorthosite-norite intrusion, AMCG affinity) contains 0.5–0.6 wt.% Mn and 1.0–3.3 wt.% Mg (Kucha and Piestrzyński, 1976); and 0.14% V for n=47 (Mikulski et al., 2022). The average content of vanadium in “sand” ilmenites is 0.202 wt.% of V_2O_5 with a low coefficient of variability of 27.17 wt.% for n = 34, similar to the ilmenites from the Krzemianka deposit with 0.25 wt.% (Mikulski et al., 2022). Several measurements showed also Al_2O_3 maximum contents close to 0.3 wt.%, Nb_2O_5 close to 0.286 wt.%, 0.131 wt.% Ta_2O_5 and ZnO up to 1.246 wt.% (Table 2).

DISCUSSION

Researchers in recent times have agreed that the rocks of the Pryazovskyi megablock of the Ukrainian Shield are the main source of minerals in the coastal deposits of the black sands of the Sea of Azov, including monazite and ilmenite. To determine the initial provenance of heavy placer minerals, all the possible sources on the Pryazovskyi megablock must be considered.

In the vicinity of the Azov Sea, the monazite is predominantly characteristic of most felsic varieties of calcium-depleted granites. It is absent from mafic and ultramafic rocks, and scarcely occurs in intermediate rocks and the most mafic varieties of gneiss, schist and migmatite (Lazarenko et al., 1981). Monazite was found in small amounts in biotite migmatites and gneisses. Among the rock complexes of the Pryazovskyi megablock, monazite is most common in the granites of the Anadolskyi, Kamianomohylskyi and Saltychanskyi complexes. It is

Table 1

Calculated ages of monazite grains from a beach of the Azov Sea, based on EMPA measurements

Point no	ThO_2	UO_2	PbO	Age (Myr)	Comment
0001	7.455	0.256	0.692	1,869	1_mnz1_1
0002	2.764	0.202	0.292	1,884	1_mnz1_2
0003	3.092	0.193	0.361	2,125	1_mnz1_3
0004	5.891	0.139	0.560	1,978	1_mnz1_4
0005	2.363	0.134	0.286	2,231	1_mnz1_5
0006	6.164	0.179	0.639	2,107	1_mnz2_1
0007	5.368	0.166	0.470	1,789	1_mnz2_2
0008	4.998	0.172	0.565	2,243	1_mnz2_3
0009	6.301	0.252	0.684	2,124	1_mnz2_4
0010	11.421	0.179	1.057	1,980	1_mnz3_1
0011	10.249	0.195	0.985	2,029	1_mnz3_2
0012	10.842	0.251	0.941	1,819	1_mnz3_3
0013	10.083	0.249	0.955	1,964	1_mnz3_4
0014	9.106	0.270	0.824	1,852	1_mnz3_5
0015	9.779	0.251	0.864	1,835	1_mnz3_6
0016	9.284	0.168	0.901	2,054	1_mnz3_7
0017	10.721	0.199	0.929	1,843	1_mnz3_8
0018	11.727	0.233	1.020	1,842	1_mnz3_9
0019	7.237	0.114	0.651	1,928	1_mnz4_1
0020	7.252	0.216	0.660	1,862	1_mnz4_2
0021	8.137	0.131	0.754	1,980	1_mnz4_3
0022	7.949	0.183	0.706	1,859	1_mnz4_4
0023	8.325	0.152	0.782	1,991	1_mnz5_1
0024	8.740	0.236	0.837	1,970	1_mnz5_2
0025	7.600	0.136	0.690	1,931	1_mnz5_3
0026	8.392	0.162	0.706	1,788	1_mnz5_4
0027	8.341	0.171	0.803	2,022	1_mnz5_5
0028	8.556	0.117	0.788	1,985	1_mnz5_6
0029	7.403	0.207	0.683	1,897	1_mnz5_7
0030	7.043	0.190	0.682	1,991	1_mnz5_8
0031	7.970	0.161	0.777	2,048	1_mnz5_9
0032	8.237	0.142	0.765	1,976	1_mnz6_1
0033	10.057	0.210	0.960	2,004	1_mnz6_2
0034	12.210	0.214	1.123	1,957	1_mnz6_3
0035	12.801	0.098	1.230	2,109	1_mnz6_4
0036	12.720	0.316	1.068	1,753	1_mnz6_5
0037	11.742	0.203	1.117	2,021	1_mnz6_6
0038	10.384	0.192	0.975	1,989	1_mnz6_7
0039	10.848	0.188	0.982	1,929	2_mnz1_1
0040	11.636	0.253	1.029	1,860	2_mnz1_2
0041	10.498	0.144	0.993	2,035	2_mnz1_3
0042	9.996	0.169	0.958	2,038	2_mnz1_4
0043	9.901	0.197	0.910	1,940	2_mnz1_5
0044	11.026	0.182	1.021	1,976	2_mnz1_6
0045	11.269	0.240	1.060	1,973	2_mnz1_7
0046	9.761	0.315	0.934	1,936	2_mnz2_1
0047	10.126	0.303	0.990	1,990	2_mnz2_2
0048	10.135	0.243	0.903	1,859	2_mnz3_1
0049	10.227	0.270	0.881	1,787	2_mnz3_2
0050	10.458	0.141	0.996	2,050	2_mnz3_3
0051	11.282	0.343	1.053	1,902	2_mnz3_4
0052	11.845	0.265	1.106	1,953	2_mnz3_5
0053	12.060	0.361	1.198	2,019	2_mnz3_6
0054	12.918	0.377	1.205	1,909	2_mnz3_7
0055	11.857	0.283	1.116	1,958	2_mnz3_8
0056	13.404	0.331	1.266	1,959	2_mnz3_9
0057	7.664	0.176	0.714	1,945	2_mnz4_1
0058	7.823	0.076	0.681	1,908	2_mnz4_2
0059	7.950	0.189	0.778	2,031	2_mnz4_3
0060	7.764	0.094	0.741	2,064	2_mnz4_4
0061	8.603	0.189	0.864	2,093	2_mnz4_5
Average	9.144	0.206	0.855	1,963	n = 61
Standard deviation	2.452	0.066	0.217	101	
Coefficient of variability	26.81	32.04	25.38		%

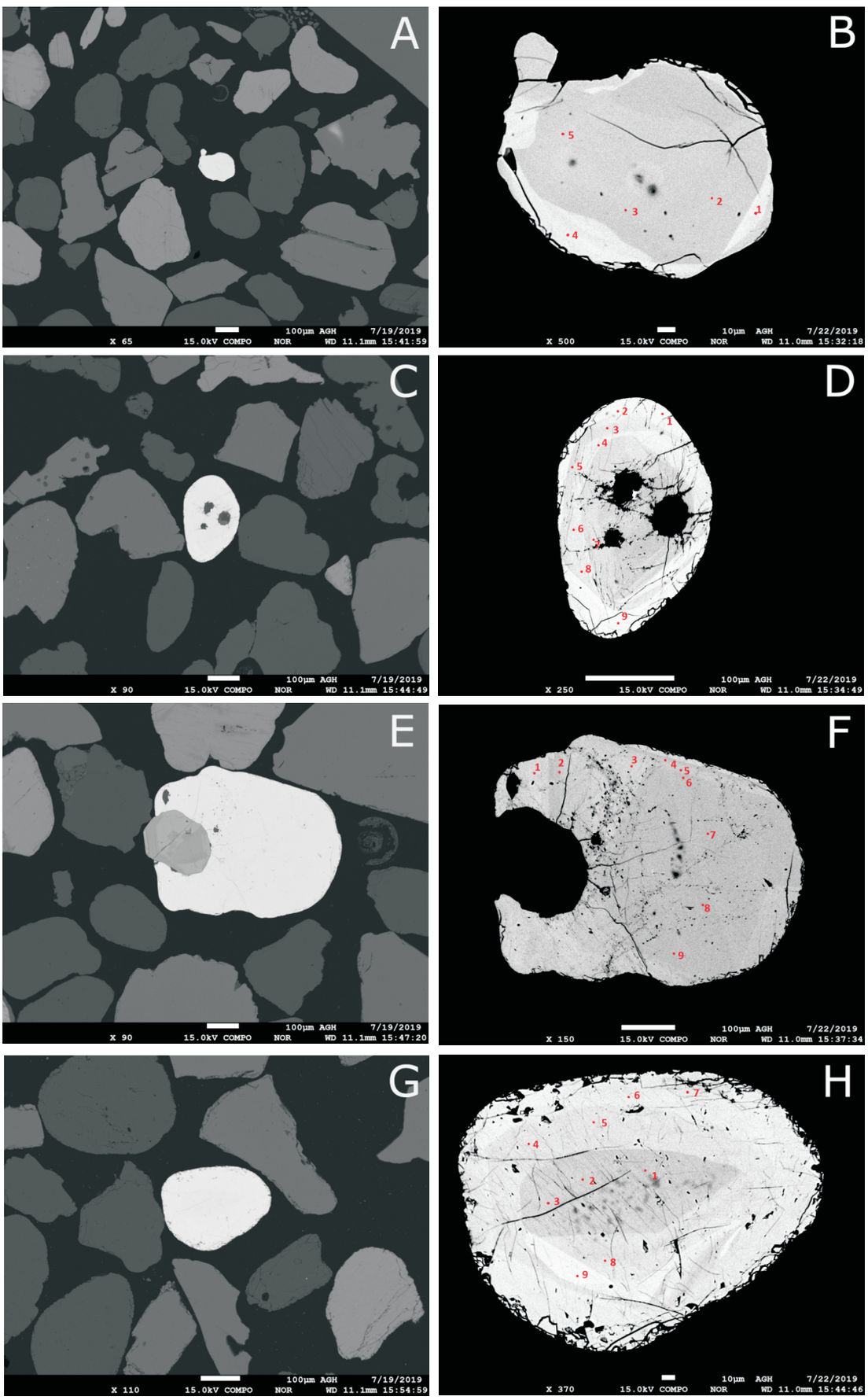

Fig. 4 A–H – back-scattered electron images: the left column (A, C, E, G) shows the typical sand association containing quartz, ilmenite, garnet, anatase, and monazite (white); the right column (B, D, F, H) shows the locations of the EMPA point analyses performed (red dots)

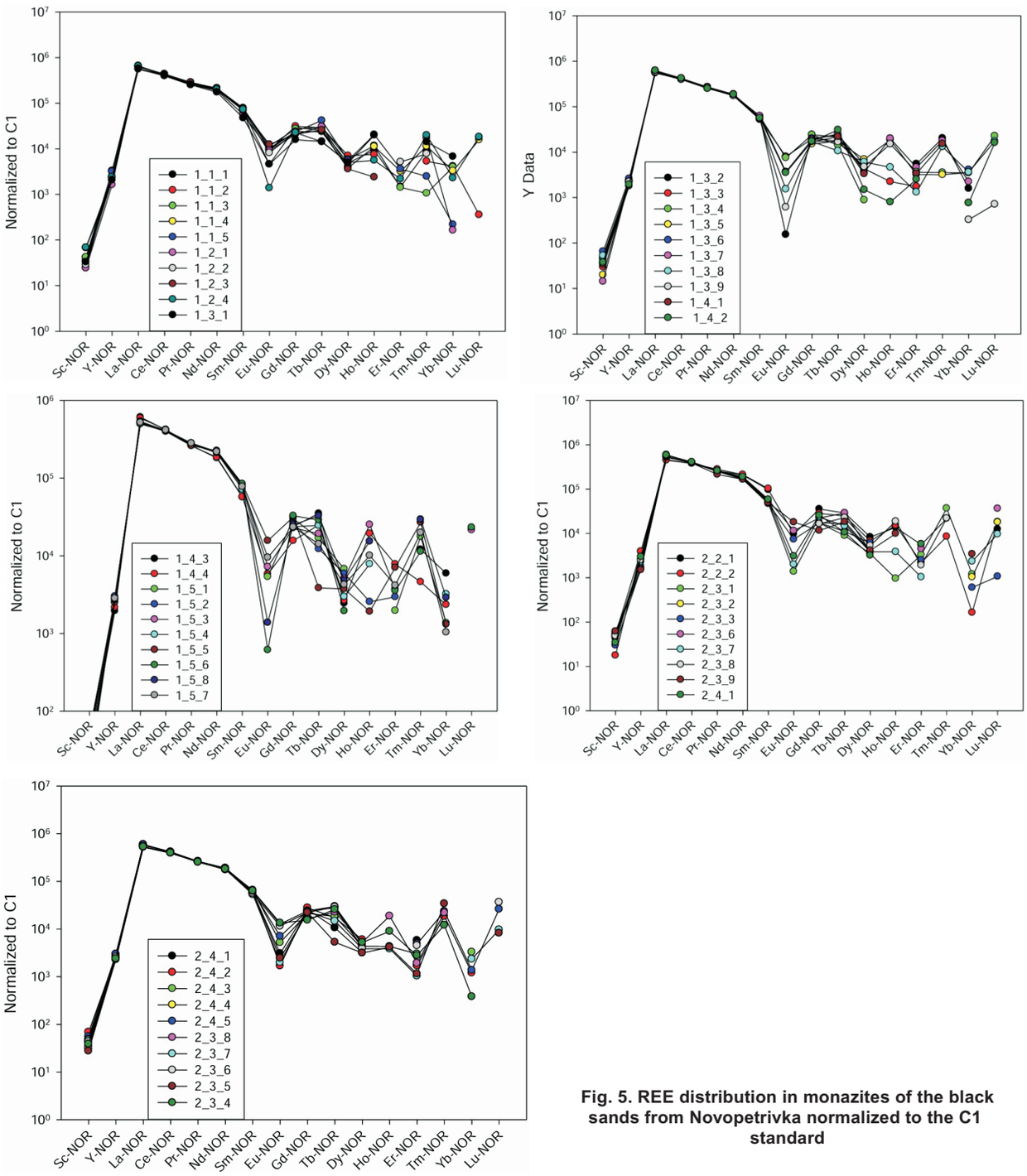

Fig. 5. REE distribution in monazites of the black sands from Novopetrivka normalized to the C1 standard

also found in widespread aplite and aplite-pegmatoid granites, pegmatites of the Central Azov Sea area, carbonatites of the Chernihivskyi complex, and migmatites and gneisses of the Zakhidnopryazovska and Tsentralnopryazovska unit. Monazite as an accessory mineral occurs in very small quantities in the rocks of the remaining complexes of the Azov Sea area (syenites, pegmatites of the Western and Eastern Azov Sea areas) (Lazarenko et al., 1981).

The monazite-rich granites of Anadolskyi complex are distributed throughout the entire Pryazovskyi megablock, and in its eastern part they form the large Anadolskyi Massif with an area of ~300 km^2 (Fig. 1). In other zones, they are represented by vein bodies occurring among gneisses and schists of the Zakhidnopryazovska and Tsentralnopryazovska units and are a part of their migmatites. Granites of the Anadolskyi complex are dated according to zircon at 2081 ±45 Myr (Shcherbak, 1995; Yesypchuk, 2004).

Saltychanskyi complex granites are medium-grained homogeneous biotite granites with the orthite form of allanite (Yesypchuk et al., 2004). A significant concentration of monazite is typical only of the allanite-poor Saltychanskyi granites from the village of Basan (Fig. 1; Lazarenko et al., 1981). The age of

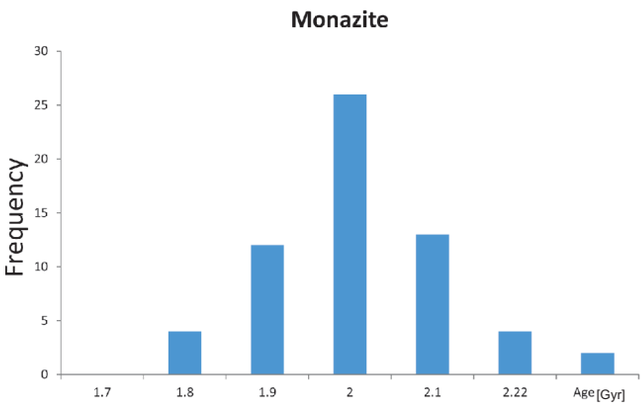

Fig. 6. Histogram of calculated monazite ages

granites of the Saltychanskyi complex, obtained from allanite, is 1960–2130 Myr, and from biotite is 1910–2135 Myr (Shcherbak, 1995; Yesypchuk, 2004; Shcherbakov, 2005).

The Kamianomohylskyi complex is represented by leucocratic porphyritic and greisenized leucogranites, thin aplite--pegmatoid, aplite-like granites and quartz porphyries. Granites form three discordant stock-like massifs: Katerynynskyi (30 km^2), Kamianomohylskyi (11 km^2), and Starodubivskyi (4.5 km^2) (Fig. 1). The age of the granites, determined by the U-Pb method, is 1808 ±18 Myr (Yesypchuk et al., 2004; Shcherbakov, 2005).

The Chernihivskyi complex is represented by alkaline rocks and carbonatites. The rocks compose the massif around the village of Chernihivka, Zaporizhzhia Oblast. They form a N–S elongated body 20 km long and up to 600 m wide. The massif lies among the plagiogranites of the Tokmatskyi complex and plagiogneisses of the Zakhidnopryazovska unit. Monazite, found in carbonatites of the Chernihivka zone, is characterized by a low content of thorium (Lazarenko et al., 1981). The age of the complex is determined by zircon from carbonatites and is 2090 ±20 Myr (Shcherbak, 1995; Yesypchuk et al., 2004).

The pegmatite fields of the Azov Sea area are developed within the domal structures of the Western Azov Sea area and are mainly associated with the granite bodies of the Shevchenkivskyi complex. In addition, among them there are pegmatites, which belong to the Remivskyi ultrametamorphic complex, as well as the Yanvarskyi and Saltychanskyi granite complexes (Isakov, 2007). The Shevchenkivskyi complex is dated by various authors within a wide range from Neoarchean

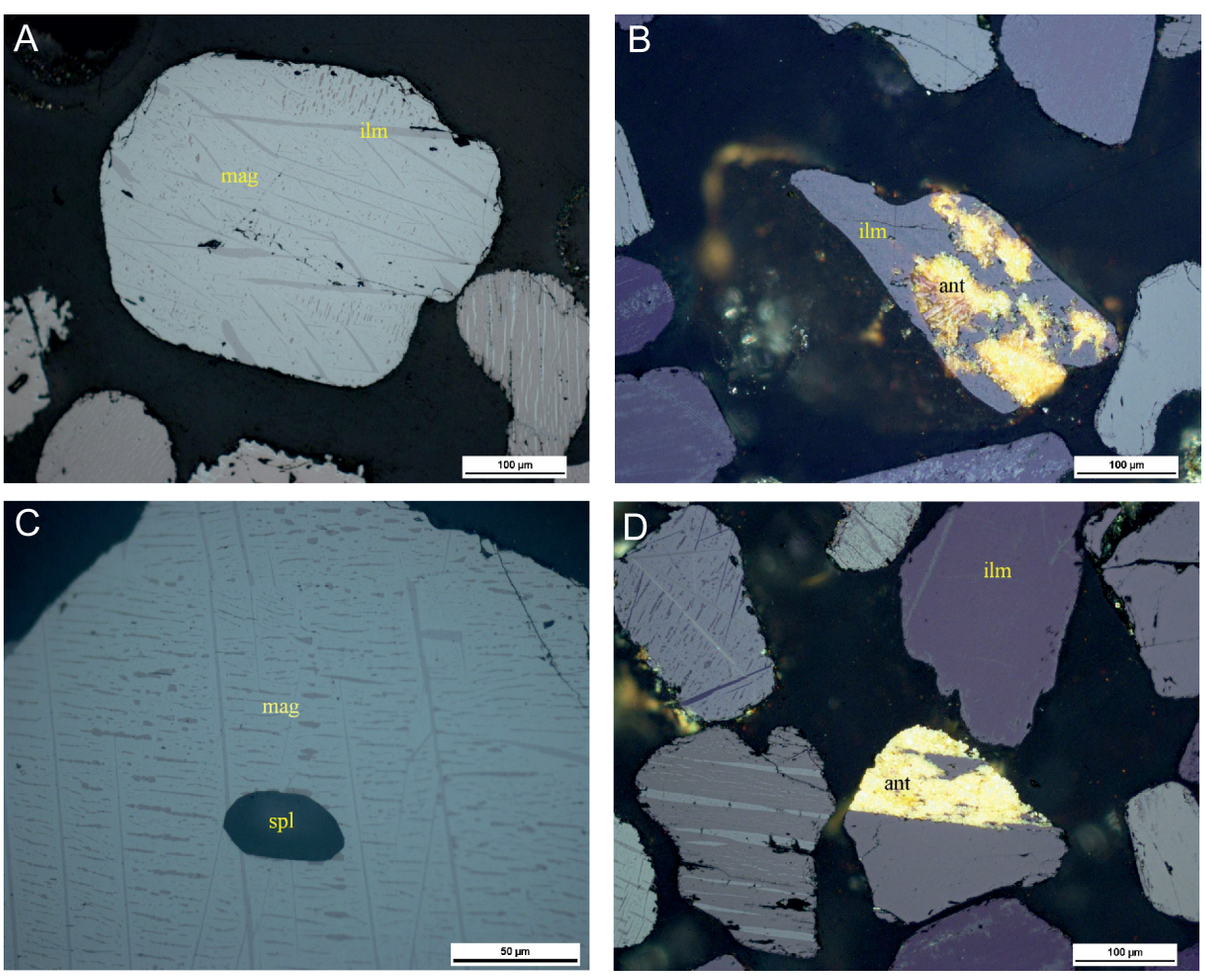

Fig. 7A – ilmenite (ilm) and magnetite (mag) grains, containing ilmenite exolutions, RL, sample 3; B – early stage of leucoxenization (ant) of ilmenite (ilm) grain, RL partly XN, sample 3; C – solid-solution ilmenite texture in magnetite (mag), spl – spinel, RL, sample 3; D – leucoxenization (ant) of ilmenite grain RL, partly XN, sample 3

Table 2

Chemical composition of ilmenites in wt.%, EMPA method

No	V_2O_5	Nb_2O_5	TiO_2	Al_2O_3	FeO	MnO	MgO	ZnO	Total	Comment
1	0.099	0.046	52.099	0.036	42.671	4.992	b.d.l.	0.19	100.174	MA.3/fot1/p1
9	0.213	b.d.l.	47.451	0.036	51.789	0.453	0.029	b.d.l.	100.008	MA.3/fot1/p4
10	0.266	b.d.l.	51.135	b.d.l.	47.678	1.888	0.027	b.d.l.	100.994	MA3/fot1/p8
11	0.131	b.d.l.	51.502	b.d.l.	45.330	3.451	0.067	b.d.l.	100.595	MA3/fot1/p9
12	0.173	0.248	51.158	0.049	45.474	2.437	0.063	0.436	100.038	MA3/fot1/p10
13	0.242	0.037	50.877	b.d.l.	46.841	2.572	b.d.l.	0.237	100.903	MA3/fot1/p3
14	0.159	b.d.l.	50.759	0.048	46.813	2.089	b.d.l.	0.102	99.970	MA3/fot1/p4
15	0.221	0.091	47.087	b.d.l.	50.190	1.294	0.178	b.d.l.	99.061	MA3/fot1/p5
16	0.323	0.038	49.940	b.d.l.	47.437	1.293	0.518	b.d.l.	99.615	MA3/fot1/p6
17	0.375	b.d.l.	52.656	b.d.l.	46.370	0.316	b.d.l.	0.102	99.849	MA3/fot1/p7
18	0.143	b.d.l.	50.813	0.196	44.334	4.493	0.645	b.d.l.	100.694	MA3/fot1/p8
19	0.233	b.d.l.	50.507	0.036	46.402	2.587	0.644	0.113	100.572	MA3/fot1/p9
20	0.214	0.045	50.896	0.211	45.623	3.319	0.133	b.d.l.	100.441	MA3/fot1/p10
21	0.249	b.d.l.	49.718	0.044	46.510	3.391	0.441	b.d.l.	100.353	MA3/fot1/p11
24	0.183	0.071	52.511	0.198	42.359	4.459	0.027	0.495	100.303	MA3/fot3/p2
3	0.240	b.d.l.	43.767	b.d.l.	53.218	3.070	0.071	0.403	97.740	MA3/fot4/p3
4	0.177	b.d.l.	50.312	0.050	46.727	2.527	0.149	b.d.l.	99.982	MA3/fot4/p4
5	0.181	0.161	49.035	b.d.l.	48.428	2.608	b.d.l.	b.d.l.	100.452	MA3/fot4/p5
6	0.145	b.d.l.	51.638	b.d.l.	45.691	1.825	0.533	b.d.l.	99.870	MA3/fot4/p6
7	0.201	0.048	51.290	b.d.l.	44.722	3.380	b.d.l.	b.d.l.	99.641	MA3/fot4/p7
8	0.161	0.203	59.994	0.300	35.729	1.145	b.d.l.	0.038	97.614	MA3/fot4p8
13	0.228	b.d.l.	51.269	b.d.l.	37.364	8.358	0.288	1.246	98.800	MA3/fot4-1/p2
15	0.180	b.d.l.	51.194	0.042	38.786	8.199	0.438	0.72	99.604	MA3/fot5/p2
17	0.253	0.070	50.818	b.d.l.	46.394	2.340	0.083	0.149	97.768	MA3/fot5/p4
19	0.294	0.046	50.405	b.d.l.	44.201	3.529	b.d.l.	0.116	98.591	MA3/fot6-1/p1
22	0.168	b.d.l.	52.986	b.d.l.	42.257	3.462	0.085	b.d.l.	98.958	MA3/fot6-1/p4
23	0.156	0.117	50.592	b.d.l.	47.857	1.141	0.173	b.d.l.	100.044	MA3/fot6-1/p6
24	0.408	0.149	53.104	b.d.l.	45.519	0.535	0.15	b.d.l.	99.920	MA3/fot6/p1
25	0.133	0.286	52.150	0.066	46.226	0.754	b.d.l.	b.d.l.	99.752	MA3/fot6/p2
26	0.104	0.102	48.785	b.d.l.	42.065	9.181	0.034	0.148	100.550	MA3/fot6/p3
28	0.223	b.d.l.	51.362	b.d.l.	46.650	1.810	0.078	b.d.l.	100.182	MA3_fot6_p4
29	0.179	b.d.l.	49.308	b.d.l.	47.099	2.506	1.047	0.174	100.389	MA3/fot6/p6
30	0.137	0.182	49.987	b.d.l.	48.225	1.027	0.028	b.d.l.	99.704	MA3/fot6/p7
S.d.	0.071	0.078	2.461	0.091	3.599	2.242	0.268	0.320	standard deviation	
Av.	0.206	0.114	50.821	0.101	45.545	2.936	0.247	0.311	average	
CV %	34.43	68.60	4.843	89.94	7.90	76.36	108.28	102.69	coeficient of variability	

Ca, SiO_2, Cr_2O_3 – sought but not detected, Sn (0.029 wt.%) was measured only for sample MA.3/fot1/p4; Ta (0.131 wt.%) was measured only for sample MA3/fot6/p3 and W (0.066 wt.%) was measured only for sample MA3/fot1/p6; b.d.l. – below detection limit

to Paleoarchean (Shcherbakov, 2005); according to the official correlation scheme, the age of the complex is 2800 Myr (Yesypchuk et al., 2004). The Remivskyi complex dates back to the Paleoarchean. The Yanvarskyi complex, which has not been officially approved, belongs to the Mesoarchean (Isakov and Shpylchak, 2013).

Thus, monazite in the rocks of the Pryazovskyi megablock of the Ukrainian Shield is predominantly characteristic of the Paleoproterozoic rocks; less commonly, it occurs in rocks of Archean age.

As a result of the radiometric analysis, it was determined that the monazite from the coastal black sands of Novopetrivka is of Paleoproterozoic age. In the Proterozoic rocks of the Pryazovskyi megablock, two separate phases of post-consolidation tectonic-magmatic activation are noted, which are dated 2.15–2.05 and 1.85–1.70 billion years. The monazites studied (see Table 1 and Fig. 6) belong to both phases. So, they could originate from the Saltychanskyi, Anadolskyi and Kamianomohylskyi complexes. Since all the monazites studied are rich in thorium, they rather do not belong to the Chernihivskyi complex.

Geographically closest to the Novopetrivka occurrences of monazite-containing rocks are the outcrops of the Kamianomohylskyi complex (1808 ±18 Myr), represented by subalkaline leucogranites (Yesypchuk, 2004). The closest to the sampling site are the Starodubivskyi and Kamianomohylskyi massifs of the Kamianomohylskyi complex. The Berda River flows through the zone of distribution of the Starodubivskyi Massif, and the left tributary of the Berda, the Karatysh River, flows across the outcrop of the Kamianomohylskyi Massif. The village of Novo-

petrivka, where the sample was collected, is located exactly at the mouth of the Berda River (Figs. 1 and 2).

But, as we can see in the histogram (Fig. 5), most of the samples studied have ages of nearly 2 billion years, thus they belong to the earliest phases of post-consolidation tectonic--magmatic activation. In this case they may have been derived from the Anadolskyi and Saltychanskyi autochthonous granitoid complexes.

Comparison of the REE content in the monazites analysed and their normalized distributions on spider diagrams with similar ones (Fig. 5) in the rocks of the Kamianomohylskyi, Anadolskyi and Saltychanskyi complexes (Fig. 8) indicates their similarity. A low Eu content in many grains from the placer deposit is also typical for the Kamianomohylskyi (Fig. 8) and Saltychanskyi complexes of the crystalline rocks. Thus, it can also be inferred that the grains with low Eu, dated at nearly 1.8 billion years, could have originated from the Kamianomohylskyi complex, and those dated at 1.9 billion years from the Saltychanskyi complex. The latter complex could also be the source of the monazites dated older than 2.1 billion years.

There has been general agreement with the views of S.V Stefanko that the Kamianomohylskyi and Anadolskyi granites could have been be the main primary source of monazites in the placers of the Sea of Azov (Stefanko, 2018). But, according to the radiometric data and the REE contents, the monazites could have originated also from the Saltychanskyi complex.

Ilmenite is a widespread mineral in the rocks of the Pryazovskyi megablock. It has been found in mafic and ultramafic rocks of the Western Azov Sea area, in calciphyres of the Temriutska suite and Osypenkivska unit, in the rocks of Oktiabrskyi alkaline massif, and in granitoids, pegmatites and carbonatites (Lazarenko et al., 1981).

The ilmenites, according to the analytical results, can be of different origins. The chemical composition of the specimens studied (Table 2) is close to the analyses published by Lazarenko (1981) representing the coastal sands of the Azov Sea spits, including the Berda spit (Fig. 1). The ilmenites of the beach zone differ from the ilmenites of the crystalline rocks of the Azov Sea area by higher average contents of MnO, usually >2 wt.% (Lazarenko et al., 1981). According to Lazarenko et al., (1981), the main source of ilmenite in the modern sediments is the volcanic rocks of the Azov Sea area. The nearest zones to the collecting site in Novopetrivka are located in the Berda River basin, where the source could be represented by the metavolcanic rocks of the greenstone Sorokynska structure, where the ilmenite-bearing Osypenkivska unit occurs. Also, titanite-bearing pegmatites are widely spread in this zone as well as in the rocks of granitoid complexes, which also contain this mineral as an accessory, namely the granites of Anadolskyi and Saltychanskyi complexes (Lazarenko et al., 1981). So, various processes could have taken place, which makes it difficult to indicate the primary sources of the ilmenite of the black sands precisely. Nevertheless, the ilmenite could well have originated from the same igneous complexes as the monazite, since monazite-bearing granites are also rich in ilmenite.

CONCLUSIONS

Radiometric age dating of monazites and the correlation of this with the geochronology of the nearby rocks indicate that the main primary sources of monazites that occur in the beach sediments in the vicinity of Berdiansk were located in the Azov

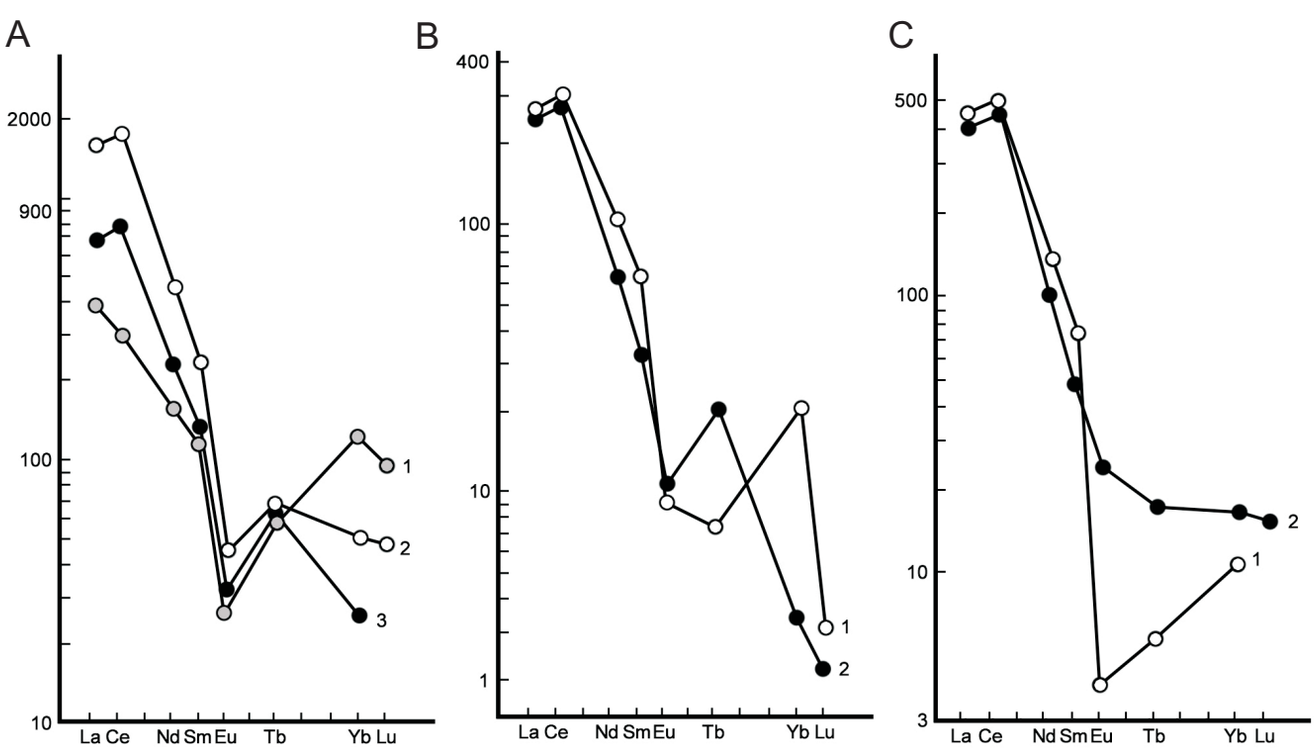

Fig. 8. REE distribution in the granites of Kamianomohylskyi (A), Anadolskyi (B) and Saltychanskyi (C) complexes (Esipchuk, 1988; Shcherbakov, 2005)

Sea area and they most probably belong to the Anadolskyi, Kamianomohylskyi and Saltychanskyi complexes of the Early Proterozoic, rather than the Chernihivskyi complex of the same age. Archean monazites, which could be linked to other units of the Pryazovskyi Megablock of the Ukrainian Shield, were not detected. The other associated heavy minerals, including ilmenite, could have been sourced also from the Precambrian rocks that occur in the Azov Sea area, namely greenstone rocks, pegmatites and granitoids.

It was also ascertained that the monazites from Novopetrivka occur in quantities indicating the possibility of them being used as a raw material for rare earth elements, especially those with MREE contents suitable for their economic development. The monazites studied from the northern zone of the Sea of Azov are characterized by significant neodymium, samarium, europium, gadolinium, terbium and dysprosium contents reaching up to 14 wt.%. The average content of neodymium in monazites is close to 10 wt.%. Apart from the monazites, ilmenite, garnet and fine grained quartz can be a good target for economic development. The data obtained could be used for further research and development of the monazite and ilmenite-bearing sands as a source of useful elements during the post-war recovery of the economy of Ukraine.

REFERENCES

Anitha, J.K., Joseph, S., Rejith, R.G., Sundararajan, M., 2020. Monazite chemistry and its distribution along the coast of Neendakara–Kayamkulam belt, Kerala, India. SN Applied Sciences, **2**, 812; https://doi.org/10.1007/s42452-020-2594-6

Chalmers, S., Zivak, D., Spandler, C., Randle, S., Walsh, J., 2024. Provenance of the Copi North heavy mineral sands deposit, Murray Basin, Australia, based on the geochronology and geochemistry of detrital zircon, rutile and monazite. Australian Journal of Earth Sciences, **71**: 1203–1222; https://doi.org/10.1080/08120099.2023.2292274

Chirvinskiy, P.N., 1925. Petrographic studies of the dark sands of the northern coast of the Sea of Azov (in Russian). Zapiski Vsesoyuznogo mineralogicheskogo obschestva, **54**: 159–172.

Dunets, V.V., Poliashov, A.S., 2014. The geological nature of the formation of placer deposits on the example of the training ground “Berda” (in Russian). Forum of Miners – 2014: materials of the international conference (Dnipropetrovsk, October 1–4, 2014). National Mining University, Dnipropetrovsk, **4**: 13–21.

Esipchuk, K.E., 1988. Petrological and geochemical foundations of formational analysis of Precambrian granitoids (in Russian). Naukova Dumka, Kyiv.

Feil, S., von Eynatten, H., Dunkl, I., Schönig, J., Lünsdorf, N.K., 2024. Inherited grain-size distributions: effect on heavy-mineral assemblages in modern and ancient sediments. Journal of Geophysical Research: Earth Surface, **129**, e2023JF007356; https://doi.org/10.1029/2023JF007356

Inozemtsev, Yu.I., 1974. Lithological and mineralogical features of the coastal marine sediments of the Sea of Azov (in Russian). Institute of Geochemistry and Physics of Minerals of the AS UkrSSR, Kyiv.

Inozemtsev, Yu.I., 1975a. Terrigenous-mineralogical provinces of the modern coastal-marine sediments of the Sea of Azov (in Russian). In: Voprosy geokhimii, mineralogii, petrologii i rudoobrazovaniya: 103–106. Naukova Dumka, Kyiv.

Inozemtsev, Yu.I., 1975b. Features of the concentration of heavy minerals on the northern coast of the Sea of Azov (in Russian). In: Voprosy geokhimii, mineralogii, petrologii i rudoobrazovaniya: 106–110. Naukova Dumka, Kyiv.

Isakov, L.V., 2007. Fields of granite pegmatites of the Western Azov Sea area (in Ukrainian). Dnipropetrovsk branch of the Ukrainian State Geological Research Institute, Kyiv.

Isakov, L.V., Shpylchak, V.O., 2013. Issues of stratigraphy and magmatism of the Western Azov Megastructure (in Ukrainian). Mineralni resursy Ukrainy, **2**: 18–23.

Itano, K., Ueki, K., Iizuka, T., Kuwatani T., 2020. Geochemical discrimination of monazite source rock based on machine learning techniques and multinomial logistic regression analysis. Geosciences, **10**, 63; https://doi.org/10.3390/geosciences10020063

Kariakin, L.I., 1948. Mineralogical composition of the Azov Sea coastal sands between Berdianskaya and Obitochnaya Spits (in Russian). Mineralogicheskiy sbornik Lvovskogo geologicheskogo obschestva, **2**: 161–174.

Khedr, M.Z., Zaghloul, H., Takazawa, E., El-Nahas, H., Azer, M.K., El-Shafei, S.A., 2023. Genesis and evaluation of heavy minerals in black sands: a case study from the southern Eastern Desert of Egypt. Geochemistry, **83**: 1–15; https://doi.org/10.1016/j.chemer.2022.125945

Kovalchuk, M.S., 2012. Beach placers of the ilmenite on the front Azov Sea (Urzuf village) (in Ukrainian). Collection of scientific works of the IGS NAS of Ukraine, **5**: 209–212.

Kucha, H., Piestrzyński, A., 1976. Investigation of some spinels and ilmenites from basic rock of NE Poland (in Polish with English summary). Mineralogia Polonica, **7**: 51–56.

Lazarenko, Ye.K., Lavrynenko, L.F., Buchinskaya, N.I., 1981. Mineralogy of the Azov Sea area (in Russian). Naukova Dumka, Kyiv.

Logvinenko, N.V., Remizov, I.N., Berger, M.G., 1964. Some features of accumulation and terrigenous-mineralogical zoning of modern sediments of the coastal zone of the Sea of Azov (in Russian). Doklady AN SSSR, **159**: 568–571.

Lozhnikov, O., Sobko, B., Pavlychenko, A., 2023. Technological solutions for increasing the efficiency of beneficiation processes at the mining of titanium-zirconium deposits. Inżynieria Mineralna, (1): 61–68; https://doi.org/10.29227/IM-2023-01-07.

Mikulski, S.Z., Sadłowska, K., Wiszniewska, J., Małek, R., 2022. Vanadium and cobalt occurrence in the Fe-Ti-V oxide deposits related to Mesoproterozoic AMCG Complex in NE Poland. Applied Sciences, **12**, 6277; https://doi.org/10.3390/app12126277

Morozewich, J., 1898. Recherches géologiques dans le district de Marioupol. Compte-rendu préliminaire (in Russian with French summary). Izvestiya Geologischeskogo Komiteta, **17**: 287–295.

Panteleyev, P.G., 1935. Ilmenite sands of the Azov Sea area (in Ukrainian). Geolohichnyi zhurnal, **1**: 75–83.

Poliashov, A.S., Khomenko, Yu.T., Chechel, P.O., 2015. Estimation of possible radiation doses on the beach sands of the Sea of Azov near the mouth of the river Berda (in Russian). Forum of Miners – 2015: materials of the international conference (Dnipropetrovsk, September 30–October 3, 2015). National Mining University, Dnipropetrovsk, **3**: 216–220.

Pyle, J.M., Spear, F.S., Wark, D.A., 2002. Electron microprobe analysis of REE in apatite, monazite and xenotime: protocols and pitfalls. Reviews in Mineralogy and Geochemistry, **48**: 337–362; https://doi.org/10.2138/rmg.2002.48.8

Savych-Zabolotskyi, K.M., 1937. Ilmenite sands of the coast of the Sea of Azov (in Ukrainian). Ucheni Zapysky Kharkivskoho Universytetu, **10**: 173–181.

Savych-Zabolotskyi, K.M., 1939. Ilmenite sands of the northern coast of the Sea of Azov (in Russian). Zapiski Vsesoyuznogo Mineralogicheskogo Obschestva, **68**: 251–254.

Shcherbak, N.P., Bratnitskiy, Ye.N., 1995. Reference isotope dates of geological processes and stratigraphic scheme of the Precambrian of the Ukrainian Shield (in Russian). Geokhimiya i Rudoobrazovaniye, **21**: 3–23.

Shcherbakov, I.B., 2005. Petrology of the Ukrainian Shield (in Russian). ZUKC, Lviv.

Shniukov, Ye.F., Orlovskiy, G.N., Usenko, P.P., Grigoriev, A.V., Gordievich, V.A., 1974. Geology of the Sea of Azov (in Russian). Naukova Dumka, Kyiv.

Shniukov, Ye.F., Inozemtsev, Yu.I., Lialko, V.I., 1983. Geology of the shelf of the UkrSSR. Solid minerals. (in Russian). Naukova Dumka, Kyiv.

Shniukov, Ye.F., Skvortsov, V.V., Permiakov, V.V., 2019. To mineralogy of dark sands of north-western coast of the Azov Sea (in Russian). Geology and Mineral Resources of World Ocean, **15**: 67–80.

Stefanko, S.V., 2018. Drains of black sands of the northern coast of the Azov Sea (in Russian). Geo-Technical Mechanics, **142**: 73–83.

Yesypchuk, K.Yu., Bobrov, O.B., Stepaniuk, L.M., Shcherbak, M.P., Hlevaskyi, Ye.B., Skobeliev, V.M., Drannyk, A.S., Heichenko, M.V., 2004. Correlation chronostratigraphic scheme of the Early Precambrian of the Ukrainian Shield (in Ukrainian). Ukrainian State Geological Research Institute, Kyiv.

Appendix 1A
Chemical composition of monazites, from Azov Sea black sand, in wt.%, EMPA measurements

No.	P_2O_5	UO_2	ThO_2	Y_2O_3	**ΣREE**	CaO	PbO	Sc_2O_3	SiO_2	As_2O_5	SO_3	Total	Comment
3	30.354	0.256	7.455	0.506	60.729	1.283	0.692	0.038	0.516	b.d.l.	0.017	101.846	1_mnz1/1/B
4	30.278	0.202	2.764	0.649	64.897	0.527	0.292	0.033	0.366	0.096	0.082	100.186	1_mnz1/2/B
5	30.456	0.193	3.092	0.668	65.198	0.522	0.361	0.038	0.412	0.033	0.056	101.029	1_mnz1/3/B
6	29.718	0.139	5.891	0.477	61.647	0.763	0.560	0.030	0.734	0.050	0.012	100.021	1_mnz1/4/B
7	30.515	0.134	2.363	0.64	61.647	0.406	0.286	0.022	0.287	0.131	0.052	100.282	1_mnz1/5/B
8	29.814	0.179	6.164	0.331	62.760	0.700	0.639	0.022	0.936	b.d.l.	0.017	101.562	1_mnz2/1
9	30.309	0.166	5.368	0.466	63.773	0.701	0.470	0.026	0.631	b.d.l.	0.064	101.974	1_mnz2/2
10	30.449	0.172	4.998	0.419	63.585	0.678	0.565	0.061	0.615	0.044	0.022	101.608	1_mnz2/3
11	30.103	0.252	6.301	0.490	62.192	0.851	0.684	0.062	0.727	0.059	0.076	101.797	1_mnz2/4
12	27.546	0.179	11.421	0.419	58.087	0.648	1.057	0.030	2.194	0.026	0.037	101.644	1_mnz3/1/D
13	28.391	0.195	10.249	0.477	58.550	0.657	0.985	0.040	1.860	0.041	b.d.l.	101.445	1_mnz3/2/D
14	28.197	0.251	10.842	0.473	58.426	0.809	0.941	0.027	1.856	0.063	b.d.l.	101.885	1_mnz3/3/D
15	28.608	0.249	10.083	0.432	58.998	0.908	0.955	0.043	1.585	0.039	0.017	101.917	1_mnz3/4/D
16	29.076	0.270	9.106	0.487	59.726	0.852	0.824	0.018	1.479	0.024	b.d.l.	101.868	1_mnz3/5/D
17	28.654	0.251	9.779	0.529	58.923	0.756	0.864	0.059	1.741	0.061	b.d.l.	101.617	1_mnz3/6/D
18	28.942	0.168	9.284	0.462	59.063	0.867	0.901	0.013	1.564	0.069	0.003	101.336	1_mnz3/7/D
19	27.637	0.199	10.721	0.441	58.016	1.214	0.929	0.048	2.043	0.044	0.050	101.342	1_mnz3/8/D
20	27.683	0.233	11.727	0.453	57.709	0.652	1.020	0.034	2.279	b.d.l.	0.014	101.804	1_mnz3/9/D
21	28.688	0.114	7.237	0.365	61.679	0.474	0.651	0.031	1.484	0.076	0.027	100.826	1_mnz4/1
22	28.716	0.216	7.252	0.395	61.772	0.469	0.660	0.034	1.559	0.061	0.014	101.148	1_mnz4/2
23	28.611	0.131	8.137	0.397	61.417	0.514	0.754	0.029	1.632	0.079	0.013	101.714	1_mnz4/3
24	28.663	0.183	7.949	0.439	61.397	0.523	0.706	0.039	1.555	0.075	0.050	101.579	1_mnz4/4
25	28.958	0.152	8.325	0.513	60.892	0.783	0.782	0.050	1.370	0.106	b.d.l.	101.931	1_mnz5/1/F
26	29.116	0.236	8.740	0.612	59.474	1.047	0.837	0.021	1.202	0.107	b.d.l.	101.392	1_mnz5/2/F
27	29.946	0.136	7.600	0.578	61.421	0.939	0.690	0.047	0.990	0.068	b.d.l.	102.425	1_mnz5/3/F
28	28.723	0.162	8.392	0.569	59.613	0.668	0.706	0.016	1.566	0.028	b.d.l.	100.443	1_mnz5/4/F
29	29.772	0.171	8.341	0.511	60.359	1.013	0.803	0.034	1.186	0.048	b.d.l.	102.238	1_mnz5/5/F
30	28.467	0.117	8.556	0.558	60.329	1.048	0.788	0.042	1.157	0.038	b.d.l.	101.1	1_mnz5/6/F
31	29.704	0.207	7.403	0.574	61.313	0.985	0.683	0.018	0.911	0.052	0.022	101.872	1_mnz5/7/F
32	29.363	0.19	7.043	0.551	60.877	0.934	0.682	0.025	0.922	0.140	0.005	100.732	1_mnz5/8/F
33	28.960	0.161	7.970	0.495	61.222	0.697	0.777	0.031	1.286	0.070	0.018	101.687	1_mnz5/9/F
34	27.753	0.142	8.237	0.460	61.368	0.698	0.765	0.054	1.808	0.055	0.271	101.611	1_mnz6/1
35	27.452	0.21	10.057	0.373	59.408	0.749	0.960	0.045	2.144	0.006	0.247	101.651	1_mnz6/2
36	26.568	0.214	12.21	0.391	56.423	0.791	1.123	0.053	2.666	0.037	0.204	100.68	1_mnz6/3
37	26.481	0.098	12.801	0.394	56.538	0.750	1.23	0.029	2.728	0.024	0.248	101.321	1_mnz6/4
38	25.491	0.316	12.72	0.399	56.951	0.822	1.068	0.043	2.714	0.031	0.205	100.760	1_mnz6/5
39	26.761	0.203	11.742	0.367	57.815	0.793	1.117	0.033	2.564	0.009	0.229	101.633	1_mnz6/6
40	26.992	0.192	10.384	0.316	59.022	0.840	0.975	0.042	2.242	0.034	0.296	101.335	1_mnz6/7
41	27.872	0.188	10.848	0.351	58.054	0.939	0.982	0.020	1.991	0.029	b.d.l.	101.274	2_mnz1/1
42	28.294	0.253	11.636	0.329	58.103	0.999	1.029	0.049	2.268	0.007	0.052	103.019	2_mnz1/2
43	27.965	0.144	10.498	0.278	58.531	0.817	0.993	0.058	2.017	0.022	0.018	101.341	2_mnz1/3
44	28.312	0.169	9.996	0.324	58.941	0.736	0.958	0.047	1.870	0.085	0.028	101.466	2_mnz1/4

45	28.342	0.197	9.901	0.309	59.148	0.781	0.910	0.019	2.008	0.038	0.032	101.685	2_mnz1/5
46	28.188	0.182	11.026	0.292	58.042	0.776	1.021	0.037	2.026	0.070	0.032	101.692	2_mnz1/6
47	27.508	0.240	11.269	0.339	57.584	0.787	1.060	0.034	2.163	0.068	b.d.l.	101.052	2_mnz1/7
48	29.863	0.315	9.761	0.794	57.187	1.609	0.934	0.048	0.950	0.046	b.d.l.	101.507	2_mnz2/1
49	29.747	0.303	10.126	0.794	56.990	1.634	0.99	0.016	1.024	0.085	b.d.l.	101.709	2_mnz2/2
50	27.551	0.243	10.135	0.370	58.655	0.737	0.903	0.052	1.998	b.d.l.	0.123	100.859	2_mnz3/1/H
51	27.300	0.270	10.227	0.319	58.821	0.812	0.881	0.045	2.154	0.027	0.161	101.017	2_mnz3/2/H
52	27.589	0.141	10.458	0.330	58.048	0.804	0.996	0.027	2.155	0.034	0.181	100.763	2_mnz3/3/H
53	26.877	0.343	11.282	0.487	57.551	0.674	1.053	0.035	2.421	0.089	0.109	100.921	2_mnz3/4/H
54	26.683	0.265	11.845	0.472	57.474	0.629	1.106	0.025	2.572	0.014	0.104	101.189	2_mnz3/5/H
55	26.459	0.361	12.060	0.527	57.019	0.621	1.198	0.039	2.705	b.d.l.	0.137	101.126	2_mnz3/6/H
56	26.608	0.377	12.918	0.463	57.029	0.637	1.205	0.042	2.859	0.088	0.123	102.349	2_mnz3/7/H
57	26.765	0.283	11.857	0.510	57.519	0.682	1.116	0.044	2.541	b.d.l.	0.155	101.481	2_mnz3/8/H
58	26.283	0.331	13.404	0.305	55.765	0.741	1.266	0.056	3.041	0.026	0.128	101.346	2_mnz3/9/H
59	29.344	0.176	7.664	0.607	60.446	0.832	0.714	0.031	1.228	0.084	0.013	101.139	2_mnz4/1
60	29.144	0.076	7.823	0.539	61.505	0.835	0.681	0.062	1.249	0.085	b.d.l.	102.009	2_mnz4/2
61	28.985	0.189	7.950	0.596	60.174	0.799	0.778	0.038	1.344	0.038	0.047	100.938	2_mnz4/3
62	29.457	0.094	7.764	0.523	60.004	0.866	0.741	0.028	1.221	0.078	0.013	100.789	2_mnz4/4
63	29.079	0.189	8.603	0.602	60.176	0.878	0.864	0.05	1.380	0.111	0.018	101.95	2_mnz4/5
Av.	28.461	0.206	9.144	0.468	59.606	0.803	0.855	0.037	1.651	0.052	0.063	101.408	n=61
S.d	1.249	0.066	2.473	0.116		0.225	0.218	0.013	0.695	0.034	0.08	0.554	n=61

Appendix 1B
REE concentrations in analysed monazites from the Azov Sea black sand, in wt%

No.	La_2O_3	Ce_2O_3	Pr_2O_3	Nd_2O_3	Sm_2O_3	Eu_2O_3	Gd_2O_3	Tb_2O_3	Dy_2O_3	Ho_2O_3	Er_2O_3	Tm_2O_3	Yb_2O_3	Lu_2O_3	ΣREE	LREE	HREE
3	15.399	28.772	2.941	11.379	1.184	b.d.l.	0.669	0.106	0.139	b.d.l.	b.d.l.	b.d.l.	b.d.l.	b.d.l.	60.729	60.374	0.355
4	17.333	30.870	3.100	11.015	1.346	0.062	0.712	0.121	0.199	b.d.l.	b.d.l.	b.d.l.	0.076	b.d.l.	64.897	64.438	0.459
5	17.921	30.855	2.967	10.973	1.320	0.075	0.624	0.123	0.165	b.d.l.	b.d.l.	b.d.l.	0.073	b.d.l.	65.198	64.735	0.463
6	15.957	29.283	2.962	11.068	1.296	0.067	0.544	0.098	0.107	b.d.l.	0.059	b.d.l.	0.068	b.d.l.	61.647	61.177	0.47
7	17.199	31.316	3.094	11.389	1.303	0.063	0.547	0.173	0.157	0.128	0.066	b.d.l.	b.d.l.	b.d.l.	61.647	64.911	0.535
8	18.010	30.070	2.770	10.107	0.976	0.060	0.476	0.126	0.113	b.d.l.	b.d.l.	b.d.l.	b.d.l.	b.d.l.	62.760	62.469	0.291
9	17.966	30.254	2.926	10.458	1.200	0.058	0.542	0.102	0.106	b.d.l.	0.094	b.d.l.	b.d.l.	0.050	63.773	63.399	0.374
10	18.336	29.616	3.087	10.576	1.189	0.081	0.476	0.107	0.102	b.d.l.	b.d.l.	b.d.l.	b.d.l.	b.d.l.	63.585	63.361	0.224
11	18.018	28.626	2.719	10.631	1.246	b.d.l.	0.518	0.059	0.142	b.d.l.	b.d.l.	0.056	b.d.l.	0.051	62.192	61.767	0.425
12	15.867	28.493	2.744	9.293	0.812	b.d.l.	0.362	0.068	0.138	0.124	b.d.l.	b.d.l.	0.124	b.d.l.	58.087	57.601	0.486
13	15.218	28.882	2.778	9.681	1.045	b.d.l.	0.551	0.089	0.118	b.d.l.	0.101	0.057	b.d.l.	b.d.l.	58.550	58.156	0.394
14	15.838	28.728	2.806	9.374	0.922	0.052	0.451	0.073	0.122	b.d.l.	b.d.l.	b.d.l.	b.d.l.	b.d.l.	58.426	58.171	0.255
15	16.277	28.483	2.736	9.563	1.052	b.d.l.	0.551	0.059	0.025	b.d.l.	0.066	b.d.l.	0.064	0.063	58.998	58.711	0.287
16	16.309	28.880	2.803	9.890	0.981	b.d.l.	0.346	0.073	0.195	0.116	0.059	b.d.l.	0.065	b.d.l.	58.426	59.209	0.517
17	15.883	28.785	2.911	9.551	1.009	b.d.l.	0.459	0.098	0.152	b.d.l.	b.d.l.	b.d.l.	0.075	b.d.l.	58.998	58.598	0.325
18	15.475	29.186	2.823	9.549	1.067	b.d.l.	0.433	0.104	0.102	0.125	0.084	0.054	b.d.l.	b.d.l.	59.726	58.557	0.506
19	15.753	28.523	2.763	9.259	0.895	b.d.l.	0.393	b.d.l.	0.171	b.d.l.	b.d.l.	b.d.l.	0.066	b.d.l.	58.923	57.596	0.42
20	15.711	28.251	2.830	9.218	0.918	b.d.l.	0.405	0.069	0.134	0.094	0.067	b.d.l.	b.d.l.	b.d.l.	59.063	57.337	0.372
21	17.109	30.010	2.941	9.993	0.949	b.d.l.	0.387	0.091	0.094	b.d.l.	b.d.l.	b.d.l.	b.d.l.	b.d.l.	58.016	61.389	0.29
22	17.299	30.207	2.709	9.897	0.961	b.d.l.	0.396	0.128	0.042	b.d.l.	0.056	b.d.l.	b.d.l.	b.d.l.	57.709	61.492	0.28
23	16.985	29.999	2.854	9.696	0.978	b.d.l.	0.547	0.146	0.069	b.d.l.	b.d.l.	b.d.l.	0.109	b.d.l.	61.679	61.059	0.358
24	16.476	30.308	2.832	9.901	0.984	b.d.l.	0.359	0.104	0.075	0.121	0.143	b.d.l.	b.d.l.	b.d.l.	61.772	60.898	0.499
25	14.551	29.454	2.977	11.483	1.329	b.d.l.	0.691	0.070	0.191	b.d.l.	b.d.l.	0.056	b.d.l.	b.d.l.	61.417	60.520	0.372
26	14.053	28.713	3.043	11.359	1.414	b.d.l.	0.604	0.051	0.167	b.d.l.	0.055	b.d.l.	b.d.l.	b.d.l.	61.397	59.186	0.288
27	14.969	29.306	3.066	11.574	1.426	b.d.l.	0.524	0.080	0.143	0.158	0.068	b.d.l.	b.d.l.	0.060	61.421	60.912	0.509
28	14.324	28.939	2.962	11.318	1.231	b.d.l.	0.545	0.102	0.084	b.d.l.	b.d.l.	b.d.l.	0.059	b.d.l.	59.474	59.319	0.294
29	14.203	28.654	2.847	12.019	1.444	0.102	0.727	0.016	0.106	b.d.l.	0.129	0.076	b.d.l.	b.d.l.	61.421	59.996	0.363

30	13.785	29.282	3.061	11.656	1.451	b.d.l.	0.753	0.120	0.055	b.d.l.	0.065	b.d.l.	b.d.l.	0.065	59.613	59.992	0.337
31	14.455	29.814	3.059	11.658	1.335	0.062	0.537	0.059	0.120	b.d.l.	0.076	0.056	b.d.l.	b.d.l.	60.359	59.992	0.393
32	14.682	29.162	3.052	11.558	1.335	b.d.l.	0.575	0.136	0.136	0.096	b.d.l.	0.083	0.053	b.d.l.	60.329	60.373	0.504
33	14.884	29.427	3.042	11.541	1.239	b.d.l.	0.669	0.122	0.200	b.d.l.	b.d.l.	0.052	b.d.l.	b.d.l.	61.313	60.820	0.402
34	17.483	30.008	2.846	9.381	0.799	b.d.l.	0.385	0.053	0.131	0.085	0.114	b.d.l.	b.d.l.	b.d.l.	60.877	60.942	0.426
35	16.999	28.759	2.717	9.344	0.836	b.d.l.	0.359	b.d.l.	0.185	b.d.l.	b.d.l.	0.084	b.d.l.	b.d.l.	61.222	59.018	0.39
36	15.871	27.353	2.586	9.149	0.902	b.d.l.	0.298	b.d.l.	0.080	0.102	b.d.l.	b.d.l.	0.063	b.d.l.	61.368	56.159	0.264
37	16.286	27.280	2.583	8.884	0.804	0.058	0.409	0.059	0.058	b.d.l.	0.090	b.d.l.	b.d.l.	b.d.l.	59.408	56.304	0.234
38	15.679	27.978	2.636	9.224	0.774	b.d.l.	0.420	0.068	0.112	b.d.l.	b.d.l.	b.d.l.	b.d.l.	b.d.l.	56.431	56.740	0.211
39	16.422	28.168	2.552	9.203	0.804	b.d.l.	0.302	b.d.l.	0.087	0.123	0.055	b.d.l.	b.d.l.	b.d.l.	56.538	57.474	0.341
40	17.125	28.593	2.563	9.092	0.857	b.d.l	0.514	0.097	0.074	b.d.l.	b.d.l.	b.d.l.	b.d.l.	b.d.l.	56.951	58.782	0.24
41	17.297	28.113	2.770	8.529	0.767	b.d.l.	0.386	b.d.l.	0.098	b.d.l.	b.d.l.	b.d.l.	b.d.l.	0.007	57.815	57.862	0.192
42	17.098	28.253	2.631	8.756	0.845	b.d.l.	0.398	0.075	0.039	b.d.l.	b.d.l.	b.d.l.	b.d.l.	b.d.l.	59.022	57.989	0.114
43	16.963	28.730	2.648	8.899	0.775	b.d.l.	0.328	0.062	0.041	b.d.l.	b.d.l.	b.d.l.	b.d.l.	b.d.l.	58.531	58.343	0.188
44	17.049	29.269	2.688	8.471	0.797	b.d.l.	0.190	0.071	0.071	0.118	0.158	b.d.l.	b.d.l.	b.d.l.	58.941	58.476	0.465
45	17.471	28.993	2.722	8.604	0.663	b.d.l.	0.444	0.062	b.d.l.	b.d.l.	b.d.l.	b.d.l.	0.053	b.d.l.	58.531	58.901	0.247
46	16.543	28.339	2.474	9.253	0.758	0.075	0.313	0.087	0.079	b.d.l.	b.d.l.	0.067	b.d.l.	b.d.l.	58.941	57.755	0.287
47	16.464	28.244	2.612	8.902	0.807	b.d.l.	0.282	0.066	0.058	b.d.l.	b.d.l.	b.d.l.	b.d.l.	b.d.l.	59.148	57.331	0.253
48	12.777	27.357	2.803	11.075	1.658	0.063	0.817	0.120	0.234	b.d.l.	0.102	0.063	b.d.l.	b.d.l.	58.042	56.550	0.637
49	12.443	27.262	3.048	11.325	1.760	b.d.l.	0.646	0.103	0.190	0.095	b.d.l.	b.d.l.	b.d.l.	0.051	57.584	56.484	0.506
50	16.328	28.810	2.701	9.263	0.821	b.d.l.	0.396	b.d.l.	0.098	b.d.l.	0.069	0.104	b.d.l.	b.d.l.	57.187	58.328	0.327
51	16.588	28.661	2.786	9.251	0.849	b.d.l.	0.397	0.069	0.110	b.d.l.	b.d.l.	b.d.l.	b.d.l.	b.d.l.	56.990	58.532	0.289
52	16.344	28.567	2.732	8.876	0.806	b.d.l.	0.397	b.d.l.	0.172	b.d.l.	0.056	b.d.l.	b.d.l.	b.d.l.	58.655	57.770	0.278
53	14.749	28.510	2.760	9.602	1.087	0.087	0.354	0.107	0.147	b.d.l.	0.055	b.d.l.	b.d.l.	b.d.l.	58.821	57.149	0.402
54	14.745	28.699	2.829	9.337	1.062	b.d.l.	0.509	b.d.l.	0.089	b.d.l.	b.d.l.	0.096	b.d.l.	b.d.l.	58.048	57.197	0.277
55	14.631	28.133	2.768	9.519	0.965	0.075	0.514	0.120	0.110	b.d.l.	0.082	b.d.l.	b.d.l.	0.102	57.551	56.605	0.414
56	14.568	28.384	2.810	9.522	0.913	b.d.l.	0.536	0.061	0.109	b.d.l.	b.d.l.	b.d.l.	b.d.l.	b.d.l.	57.029	56.746	0.283
57	14.822	28.392	2.800	9.708	0.962	b.d.l.	0.378	0.094	0.149	0.117	b.d.l.	0.062	b.d.l.	b.d.l.	57.019	57.062	0.457
58	15.19	27.822	2.331	8.875	0.846	0.117	0.267	0.076	0.116	b.d.l.	b.d.l.	b.d.l.	0.063	b.d.l.	57.029	55.448	0.317
59	16.193	29.463	2.823	10.114	1.009	b.d.l.	0.584	b.d.l.	0.090	b.d.l.	0.106	b.d.l.	b.d.l.	b.d.l.	57.519	60.206	0.24
60	16.589	29.867	2.870	10.102	1.082	b.d.l.	0.638	0.072	0.169	b.d.l.	b.d.l.	0.062	b.d.l.	b.d.l.	55.765	61.159	0.346

61	16.316	29.5	2.777	9.596	1.122	b.d.l.	0.488	0.076	0.123	b.d.l.	0.055	b.d.l.	0.060	b.d.l.	60.446	59.833	0.341
62	15.963	29.531	2.754	9.81	1.053	0.083	0.551	0.124	0.135	b.d.l.	b.d.l.	b.d.l.	b.d.l.	b.d.l.	61.505	59.745	0.259
63	16.114	29.224	2.760	9.944	1.052	b.d.l.	0.550	0.116	0.117	b.d.l.	0.089	0.066	b.d.l.	0.073	60.174	59.69	0.486
Av.	15.989	28.974	2.813	9.971	1.05	0.032	0.482	0.082	0.118	0.04	0.046	0.029	0.028	0.014	59.606	58.180	0.356
S.d	1.284	0.873	0.164	0.975	0.24	0.03	0.132	0.034	0.046	0.047	0.039	0.028	0.03	0.025	n= 61		
CV	**8.01**	**3.01**	**5.83**	**9.77**	**22.85**	**93.75**	**27.38**	**414.63**	**256.52**	**117.50**	**84.78**	**96.55**	**107.14**	**178.57**	%		

CV – coefficient of variability, b.d..l. – below detection limit, S.d – standard deviation